Effects of ion-beam bombardment on the physical properties of 100Cr6 steel

R. Droppa Jr[1], H. Pinto[2], J. Garcia[3], E. Ochoa[4], M. Morales[4], S. Cucatti[4], and F. Alvarez[4]

[1]Centro de Ciências Naturais e Humanas - Universidade Federal do ABC, Santo André, Brazil
[2]Escola de Engenharia de São Carlos - Universidade de São Paulo, São Carlos, Brazil
[3]Sandvik Machining Solutions, Stockholm, Sweden
[4]Instituto de Física ‘‘Gleb Wataghin" - Universidade Estadual de Campinas, Campinas, Brazil

Abstract

The effect of ion-beam bombardment on the physical properties of 100Cr6 steel is reported. The energy dependence of the in-depth stress and the pattern formation are presented. The modified region by the relative low energy (< 1keV) ions extend orders of magnitude deeper than the stopping region of the projectiles. The formation of peculiar patterns on the treated surface is explained by the current model of surface instability created by preferential sputtering and surface diffusion in metals.

Keywords: Surface modification, ion-beam bombardment, Internal stresses

1. Introduction

The development of new processes to improve the adhesion and wear resistance of hard coatings in cutting tools and moulds is a challenging task. Such processes aim to modify the surface of the substrate at atomic level by forming new phases, controlling internal stress, and/or tailoring the surface topography. The pre-treatment of steel surfaces by using heavy ions bombardment and posterior N^+ ion beam nitriding process could thus be used to get surfaces suitable prepared for hard coatings deposition improving the well-known “duplex” process. This paper focuses the research on the stress and topography generated by heavy ions bombardment of different energies on 100Cr6 steel.[1] The in-depth stress study shows that the bombardment effect extend much deeper than the damaged region. Changes from compressive to tensile stress are also observed.

2. Experiments

The 100Cr6 steel is a high carbon, chromium containing low alloyed steel used in ball bearings or other applications where resistance to fatigue is demanded. The studied samples are 20 mm diameter disks, 2 mm thick, sliced from the same rod (C:1.00; Si 0.25; Mn 0.35; Cr 1.50 %wt) and mirror polished. The studied samples were bombarded perpendicularly to the free sample surface with Xe^+ ions at different kinetic energies (0.2 keV to 1.0 keV). The bombardment of the samples was performed in an IBAD system with x-ray electron spectroscopy (XPS) for *in situ* studies. Details of the apparatus are reported elsewhere.[2] Prior to Xe^+ bombardment, the samples were sputter cleaned by Ar^+ ion bombardment (0.6 keV) during 5 minutes. This ensured identically starting substrates surface. The Xe^+ bombardment treatment was performed at room temperature during 30 minutes. The sample temperature was monitored by a thermocouple fixed in the sample holder and maintained below 300°C. The base pressure of the chamber was $<1.1 \times 10^{-4}$ Pa and the working pressure maintained at $\sim 1.2 \times 10^{-1}$ Pa during ion bombardment. The Xe concentrations underneath the samples surfaces were obtained *in situ* by XPS analysis. The layer probed is around ~5Å depth.[3] Ion implantation simulation using TRIM shows that the average projectile penetration region is

around 11-18 Å, i.e., approximately the same range probed by XPS.[4, 5] The samples were further analyzed by Grazing Incidence X-ray Diffraction (GIXD) at different incident angles in order to obtain information about the average residual stress gradient induced by the bombardment treatment. These measurements were performed at the XRD1 beamline of the Brazilian Synchrotron Light Laboratory (LNLS). The x-ray wavelength used in the experiment was 1.7701 Å. A Ge (111) crystal analyzer was used on the 2θ diffractometer arm to improve the instrument resolution and to make the measurements insensitive to small sample misplacements as well as to possible geometrical aberrations.[6] The residual stress depth profiling was performed by using the $\sin^2\psi$ method in the asymmetric multi-reflection mode (fixed grazing incidence angle).[7] The effective penetration depth for each x-ray incidence angle was calculated according to Noyan[8], assuming a layer of material contributing to 63% to the diffracted intensity. Atomic force microscopy (AFM) was utilized in the analysis of the surface patterning.

3. Results and analysis

3.1 Structure

Figure 1, left, shows the XRD diffractogram of the 100Cr6 steel pristine sample. The characteristic reflections associated to α-Fe (ferrite) and Fe_3C (cementite) are indicated.

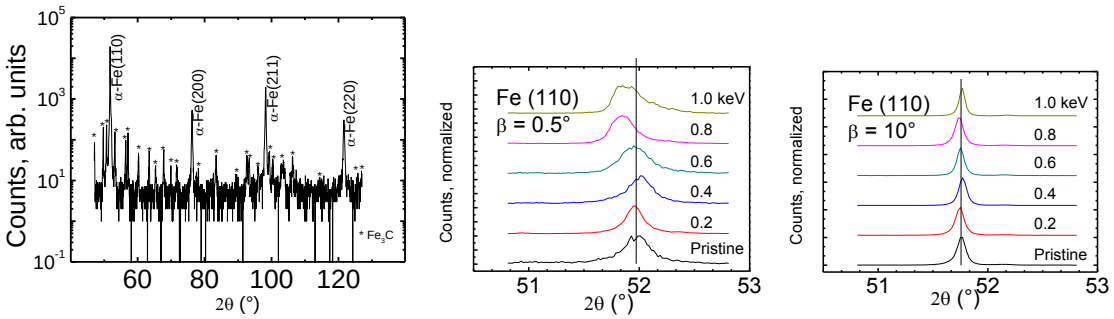

Figure 1. Left: θ–2θ diffractogram of a typical sample. Middle: α-Fe (110) x-ray diffraction peak for different Xe beam energies, taken at incident beam angle β=0.5°. Right: incident beam angle β=10°.

Figure 1 (middle and right) shows examples of the α-Fe (110) diffraction peak profiles of each sample after Xe^+ ion bombardment taken at two incident x-ray beam angles β (0.5° and 10°). The curves show a shift of the diffraction lines after ion energy bombardment relative to the non-bombarded sample. This is compatible with a non-uniform lattice deformation as a function of the projectile energy. The shift to the right, corresponding to a lattice shrinking, is found only at 0.4 keV ion bombardment energy, i.e., just the energy giving the highest Xe concentration retained in the samples as obtained from the XPS analysis (Figure 2, inset). For all other bombardment energies the lattice is stretched, as the diffraction lines shift to lower reflection angles. For an incident angle of β=0.5° the depth probed by the x-rays is ~ 0.2 μm. This corresponds to a layer whose thickness is much larger than the stopping distance of the projectiles (≤18 Å).

We note that for the highest bombardment energies the reflections associated with the most external atomic layers (≤ 0.2 μm) display asymmetric profiles suggesting the formation of a new distorted phase. These asymmetries also appear in the diffractograms for other reflections associated with the α-Fe phase (not shown). On the other hand, for an incident angle of β=10° the depth probed by the x-ray is ~ 3.4 μm. As observed in Figure 1 (right) the reflection lines

are practically not affected by the bombardment, in opposition to the top most layers, where the Xe^+ ion bombardment generates strong strain/stress (Figure 1 left).

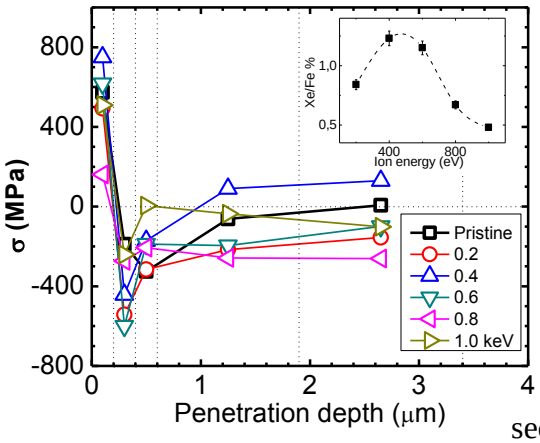

Figure 2. In depth stress distribution in the steel samples. The dotted vertical lines indicate the layers according to the model of constant average stress discrete layers used to deconvolute the stress profile. Here, each point represents the average stress in the respective layer. Inset: Xe/Fe (%) ratio for each bombarded sample as a function of ion energy.

Figure 2 shows the deconvoluted stress profile for the studied bombardment energies. As observed, all samples show a ~ 0.2 μm layer under tensile stress. Beneath this layer there is a second layer of same thickness under compressive stress. In agreement with the results discussed above, the maximum tensile stress is obtained for the sample bombarded with 0.4 keV and having the maximum Xe/Fe ratio retained in the material. Furthermore, for all bombardment energies, there is the formation of a thin compressive stressed layer just below the top most surface layer.

3.2 Morphology

The surface patterns and roughness of the bombarded samples are also affected by the bombardment as illustrated by the AFM micrographs (Figure 4, left). For the sake of clarity only the micrographs of a particular sample is displayed. As observed in Figure 4 (right) the Xe^+ ion bombardment also increases the roughness, generating a characteristic pattern on the material surface. For the highest studied bombardment energy the roughness and the sputtering yield seems to decrease. Nevertheless, more experimental data are necessary to confirm this result. Also, Figure 4 (right) suggests that there is a slope change for higher energies than 0.4 keV, just the energy where the Xe/Fe ratio is maximum (Figure 2, left).

The treated surfaces show characteristic patterns at different bombardment energies. It is particularly interesting the 1.0 keV case where pyramidal patterns are observed (Figure 4, left). This peculiar topology appears in some grains on the treated surface suggesting that they own similar crystallographic orientations relative to the ion beam.

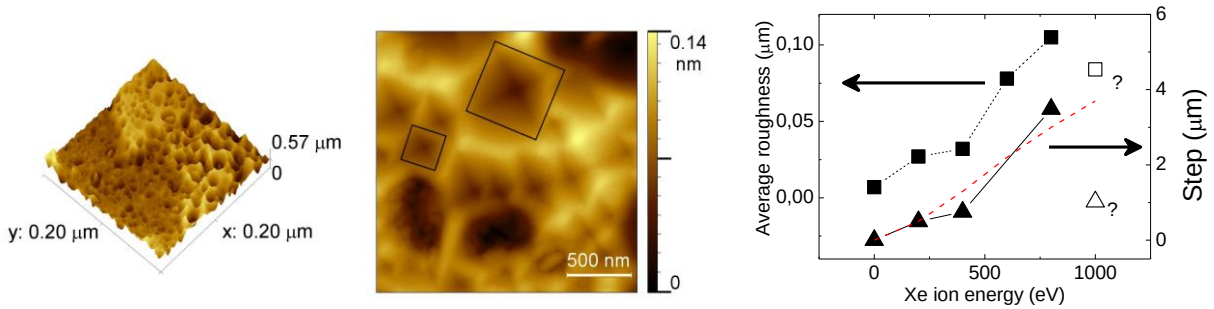

Figure 4. Left: AFM micrographs from the 1 keV bombarded sample. The pyramidal groove patterns are distinguished. Right: Roughness (squares) and step (triangles) formed on the bombarded surfaces as a function of Xe energy. The red dashed curve is the theoretical calculation for step formation according to the Xe sputtering yield for 100Cr6 steel.

This behavior is explained by the roughening instability model due to Ehrlich-Schwoebel diffusion barriers in metal.[9] Roughly speaking, the regular pattern stems from essentially two mechanisms inducing surface instability. The first one is related to the surface curvature dependence of the ion sputtering and the second one is due to the presence of an energy barrier to diffusing adatoms to descend step edges. Also, the 4-fold symmetry of the patterns suggests that these grains are oriented in the <100> direction.

4. Conclusions

X-ray experiments show that the bombarded Fe matrix changes from tensile to compressive stress in a layer close to the bombarded surface (< 400 Å) but much more profound than the stopping range of the projectiles (< 18 Å). In this region, also, a lattice crystalline deformation and the upsurge of new phase(s) is (are) noticeable. At deeper distance from the material surface, the stress diminishes and extends at least up to ~3.4 μm. The only peculiar behavior is observed in the samples bombarded with 0.4 keV switching from compressive to tensile stress again. It is remarked that at this particular energy the sample retains the highest relative Xe atoms concentration. Moreover, at this energy, the projectiles induce the maximum strained/stressed surface structure observed in this study. In conclusion, the generated compressive stress depends on the projectile energy and it extends orders of magnitude deeper than the stopping range of the ions being ~11-18 Å. The process of sputtering and surface diffusion probably explains the formation of patterns as those reported in noble gases metals bombarding studies.[9]

The roughness increasing on energy of Xe^+ ions bombardment augments the sample surface effective area. This effect probably contributes to increase nitrogen retention in nitriding experiments influencing the diffusion process by augmenting the chemical potential at the sample surface. The surface modification to atomic level by ion bombardment to improve hard coatings adhesion could be a route to increase cutting tools performance.

Acknowledgements

Part of this work was supported by FAPESP, project 05/53926-1. FA and EO are CNPq fellows. The authors are indebted to C. Piacenti for technical help. The XRD measurements were performed at the XRD-1 beamline of LNLS. The AFM measurements were performed at the Multiuser Experimental Center of UFABC.

References

[1] Standard ASTM A 295/1994.
[2] P. Hammer, N. M. Victoria, F. Alvarez, J. Vac. Sci. Technol. A 16, 2491 (1998).
[3] D. Briggs and M. P. Seah, *Practical Surface Analysis*, 2nd ed. Willey,New York, **1** (1993).
[4] J.P.B. Biersack, G. L. Haggmark, Nucl. Instrum. Methods 174 (1980) 257.
[5] E.A. Ochoa, C.A. Figueroa, T. Czerwiec, F. Alvarez, Appl. Phys. Lett., **88** (2006) 254109.
[6] P. J. Withers, M. Preuss, P. J. Webster, D. J. Hughes, A. M. Korsunsky, Mat. Sci. Forum 404-407, 1 (2002).
[7] Quaeyhaegens, C., Knuyt, G. & Stals, L. M. Surf. Coat. Technol. 74–75, (1995) 104–109.
[8] I.C. Noyan, J.B. Cohen, Residual Streess-Measurement by Diffraction and Interpretation, Springer-Verlag, Berlin, 1987.
[9] See W. L. Chana and E. Chason, J. of Applied Phys.**101** (121301) 2007 and references there in.